Theoretical Study of Proton Transfer in Hypoxanthine Tautomers: Effects of Hydration

M. K. Shukla[†,‡] and Jerzy Leszczynski*[,†]

Computational Center for Molecular Structure and Interactions, Department of Chemistry, Jackson State University, 1400 J.R. Lynch Street, Jackson, Mississippi 39217 and Department of Physics, Banaras Hindu University, Varanasi-221005, India

Received: November 17, 1999; In Final Form: January 14, 2000

Computational investigations on the proton transfer in the isolated, monohydrated, and dihydrated forms of hypoxanthine have been performed. Ground state geometries were optimized at the HF/6-31G(d,p), HF/6-311++G(d,p), and MP2/6-31G(d,p) levels of theory while those of the transition states corresponding to the proton transfer from the keto to the enol form of the molecule were characterized at the HF/6-31G(d,p), HF/6-311++G(d,p), MP2/6-31G(d,p)//HF/6-31G(d,p), and MP2/6-311++G(d,p)//HF/6-311++G(d,p) levels of theory. It is found that, in the gas phase, the molecule would exist mainly in the keto prototropic forms. The transition states corresponding to the proton transfer from the oxo to the hydroxy form for the mono- and dihydrated forms were found to have a zwitterionic structure; the geometries are more easily expressed in the form of $H_3O^+\cdots HX^-$ for the monohydrated forms and $H_5O_2^+\cdots HX^-$ for the dihydrated forms of the molecule.

Introduction

Proton transfer deals with bond-breaking and bond-forming phenomena in chemical and biological systems. Such phenomena are believed to induce the formation of rare tautomers of nucleic acid bases. These rare tautomers are suggested to be responsible for mutation by inducing mispairing of nucleic acid bases.[1] A large number of theoretical and experimental studies have been performed to enrich the information regarding the possible mechanism of formation of rare tautomers, their properties, and the possible effects of environments on the tautomeric equilibria.[2] Hypoxanthine (HX), a purine derivative, is an intermediate of purine catabolism in living systems.[3] It can form by deamination of guanine and is found as a minor purine base in transfer RNA.[4]

Different experimental and theoretical techniques have been applied to study the relative stability of different tautomers of HX.[5−12] Hernandez et al.[5] have carried out HF/6-31G(d) level of geometry optimization calculations and single point electron correlation (MP2/6-31+G(d,p)) and DFT B3LYP calculations on the different tautomers of HX in the gas phase. Their results suggest that in the gas phase HX can exist mainly in two keto tautomeric forms, N1HN7H and N1HN9H, the former being the dominant species. Similar results have also been found at the DFT level of theory using the Becke−Perdew functional and the DZVP basis set.[9] At the HF/6-31G(d) and HF/6-31G-(d,p) level of theory, both forms (keto-N1HN7H and keto-N1HN9H) are found to have approximately similar stability in the ground state,[5,6] while for the MIDI basis set, the keto-N1HN9H form is found to be about 5 kJ/mol more stable than the keto-N1HN7H form.[6] Hernandez et al.[5] have predicted that in the gas phase a small amount of the enol-N9H form of HX may also be present. On the basis of the relative stability of these tautomers at the MP2/6-31+G(d,p)//HF/6-31G(d) level of theory, they have proposed that in the gas phase the populations of the keto-N1HN7H, keto-N1HN9H, and enol-N9H tautomers would be around 81%, 18%, and 1%, respectively.[5] An IR spectroscopic study of HX in the Ar matrix suggests the presence of about 5% of the enol form of the molecule.[7] Ultraviolet photoelectron spectra of HX indicate that the keto-N1HN7H tautomer is more stable than keto-N1HN9H form in the gas phase.[8] Theoretical calculations show that under aqueous solvation, the enol-N9H form is largely destabilized with the keto-N1HN9H form being more favored than the keto-N1HN7H form.[5] In crystal, HX occurs as the keto-N1HN9H tautomeric form.[13] The UV spectroscopic study in an aqueous medium also indicates the dominance of the keto-N1HN9H form over the keto-N1HN7H form.[14] An NMR spectroscopic study in dimethyl sulfoxide indicates that the keto-N1HN7H form is more favored.[15] In the case of xanthine, a dioxypurine, the keto-N7H form is predicted to be the dominant tautomer present in the gas phase and in aqueous media.[2h,i]

The above discussion suggests that there are controversies concerning the stability and existence of different tautomeric forms of HX and its tautomerism should be studied at the reliable electron correlation level of theory. Furthermore, to the best of our knowledge, the study of tautomerization barrier heights, the transition state corresponding to the proton transfer from the keto to the enol form of the molecule, and the effects of hydration on the tautomeric equilibria and on the nature of the transition states have yet not been performed. The effect of hydration is important in view of the reported fact that the solvation of DNA is very local in the first solvation shell; only a limited number of water molecules contribute to it.[16] The present study has been undertaken with the objective to adhere to the following questions: (1) What is the effect of hydration on the relative stabilities of different tautomers and their geometries? (2) What is the structure of the transition state corresponding to the keto−enol tautomerism and the effect of hydration on the nature of transition states? (3) What is the barrier height for the keto−enol tautomerization and the

[†] Jackson State University.
[‡] Banaras Hindu University.

10.1021/jp9940912 CCC: $19.00
Published on Web 03/10/2000

influence of hydration on the barrier height? (4) What is the interaction energy of the hydrated complexes of different tautomers?

Computational Details

Ground state geometries of the tautomers and their mono- and dihydrated complexes were optimized using the ab initio Hartree−Fock method applying the 6-31G(d,p) and 6-311++G(d,p) basis sets and subsequently the second order of the Moller−Plesset (MP2) perturbation theory applying the 6-31G(d,p) basis set. All geometries of local minima and transition state were optimized without any symmetry restrictions (C_1 symmetry was assumed). Transition state geometries were optimized using the option OPT = (TS, CALCHFFC, NOEIGENTEST) at the HF/6-31G(d,p) and HF/6-311++G(d,p) levels of theory. The keyword OPT = TS performs the transition state (first-order saddle point) geometry optimization using the Berny algorithm. By default the Berny optimization program checks the number of negative eigenvalues of the Hessian at each step of the transition state optimization and if the number is not correct (1 for a transition state), the job is aborted. This test is suppressed by using the option NOEIGENTEST. The option OPT = CALCHFFC is used to compute the analytic HF force constants at the first point of transition state geometry optimization. Single point calculations for the transition state geometries were also performed at the MP2/6-31G(d,p)//HF/6-31G(d,p) and MP2/6-311++G(d,p)//HF/6-311++G(d,p) levels of theory. It is well-known that a linear scaling to the zero point vibrational energy (ZPE) is necessary for the ZPE corrected total energy. A scaling factor of 0.9135 has been suggested for the HF/6-31G(d) level of theory while 0.9676 has been suggested for the MP2(fc)/6-31G(d) level of theory.[17] Here we have used a scaling factor of 0.9135 for the HF method at both 6-31G(d,p) and 6-311++G(d,p) basis sets and 0.9676 for the MP2/6-31G(d,p) level of calculations. The characteristics of the local minima and transition states were verified by estabilishing that the matrixes of the energy second derivatives (Hessian) have zero and one negative eigenvalues, respectively. The equilibrium constant was calculated using the standard formula $K = e^{-\Delta G/RT}$, where the calculations were performed at $T = 298.15$ K. All these calculations were performed using the Gaussian 94 program.[18]

Results and Discussion

Geometry and Relative Stability, In the present study, the four tautomers of hypoxanthine, namely keto-N9H, keto-N7H, enol-N9H, and enol-N7H, were considered as they are expected to contribute in different ratios.[5−15] In these tautomers, hydrogen is attached at the N1 site of the molecule. These enol tautomers are of cis type, because the H atom attached to the CO group is in cis configuration with respect to the N1 atom (likewise, in the trans the H atom of OH is in trans configuration with respect to the N1 atom). These configurations (cis type) are more stable than the respective trans configurations.[5,9] The geometrical consideration of the enol-N7H form explains the lower stability of its trans configuration than that of the cis configuration, while the higher basicity of the N1 site than N7 site has been speculated from the higher stability of the *cis*-enol-N9H (enol-N9H) configuration than the trans configuration.[9] This speculation is also supported from a recent B3LYP/6-31+G(d,p) computation[2j] in which the proton affinity of the N1 site of adenine is predicted to be more than the proton affinity of the N7 site. The optimized geometric parameters for these tautomers at the HF/6-31G(d,p) and HF/6-311++G(d,p) levels of theory were found to be similar; therefore, only the geometries at the MP2/6-31G(d,p) and HF/6-311++G(d,p) levels of theory are presented in Figures 1 and 2. The geometric parameters for the mono- and dihydrated complexes of these tautomers in the hydrogen-bonding region at the same level of theory are also presented in these figures. Data shown in Figures 1 and 2 exhibit that hydration slightly influences the shortening of the N1C6 bond and the lengthening of the CO bond for the keto forms while the reverse is true for the enol tautomers. Such phenomena can be attributed due to hydrogen bond accepting and donating properties of the oxo and hydroxy groups, respectively, of the molecule. All other geometrical parameters are almost unaffected by hydration; therefore, they are not shown in these figures. Thus, the influence of the interaction of one or two water molecules on the geometries of the tautomers is localized mainly in the region of intermolecular hydrogen bonding (Figures 1 and 2). It is also found that the inclusion of electron correlation (MP2) predicts stronger intermolecular hydrogen bonding even at the comparatively smaller basis set than at the HF level of theory (Figures 1 and 2).

The relative total energies and the free energies of the isolated and hydrated tautomers of HX at the HF/6-31G(d,p), MP2/6-31G(d,p), and HF/6-311++G(d,p) levels of theory are presented in Table 1. The sequence of relative stability of the isolated tautomers can be written in the following order.

$$\text{keto-N7H} \approx \text{keto-N9H} > \text{enol-N9H} > \text{enol-N7H}$$

In the case of hydrated tautomers, the relative stability for the monohydrated tautomers can be written as

$$\text{keto-N9H}\cdot H_2O \approx \text{keto-N7H}\cdot H_2O > \text{enol-N9H}\cdot H_2O > \text{enol-N7H}\cdot H_2O$$

while those for the dihydrated tautomers is

$$\text{keto-N9H}\cdot 2H_2O \approx \text{keto-N7H}\cdot 2H_2O > \text{enol-N9H}\cdot 2H_2O > \text{enol-N7H}\cdot 2H_2O$$

Thus, for the isolated tautomers the keto-N7H form is predicted to be slightly more stable than the keto-N9H form at both the HF and MP2 levels of theory in the gas phase (Table 1). Therefore, both of these forms would coexist in the gas phase. The enol-N9H form, being only ~3.0 kcal/mol less stable at the MP2/6-31G(d,p) level of theory, would also be present in the gas phase. Also, in earlier works,[5,6,8,9] both of the keto forms have been reported to be in coexistence with each other. The predicted stability of the enol-N9H form by us is validated from the matrix isolation study of HX[7] in which the enol form is shown to be present in about 5% of the total tautomeric forms of the molecule.

Hydration slightly favors the stability of the keto-N9H form over the keto-N7H form. Hernandez et al.[5] have modeled the effect of aqueous solvation on the tautomeric equilibria of HX using a continuum approach and have shown that while in the gas phase the keto-N7H form of HX is the most stable, in aqueous media it is destabilized. Subsequently, the keto-N9H form is more or approximately equal in stability to the keto-N7H form depending on the method used in the computation. Accordingly, at the AM1-SM2 and AM1-MST levels, the keto-N9H form is about 0.7 and 0.1 kcal/mol more stable than the keto-N7H form while at the MST(6-31G(d)) level, the keto-N7H tautomer is about 0.2 kcal/mol more stable than keto-N9H form; in the gas phase the corresponding stability was 0.9 kcal/mol at the MP2/6-31+G(d,p)//HF/6-31G(d) level.[5] A shift of

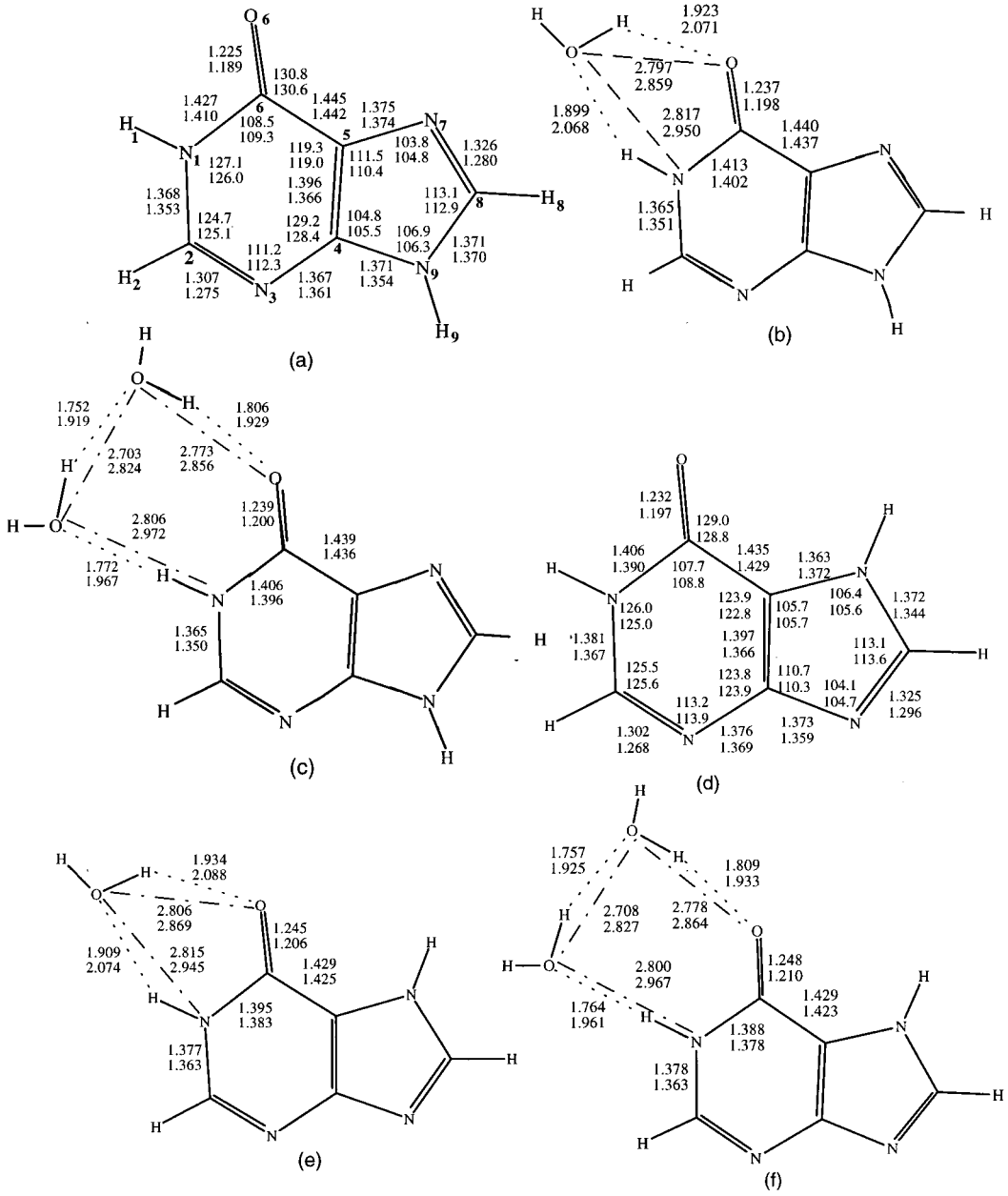

Figure 1. MP2/6-31G(d,p) (top index) and HF/6-311++G(d,p) (bottom index) geometries of hypoxanthine tautomers and hydrated complexes: (a) keto-N9H, (b) keto-N9H·H_2O, (c) keto-N9H·$2H_2O$, (d) keto-N7H, (e) keto-N7H·H_2O, and (f) keto-N7H·$2H_2O$. Bond lengths are in angstroms and bond angles are in degrees.

tautomeric equilibrium has been reported earlier for other nucleic acid bases and other prototypes of the molecules.[19,20] To the best of our knowledge, no experimental study exists for the hydration of HX. However, the experimental study of hydration of some derivatives of pyridine and pyrimidine are available, and they show the shift in tautomeric equilibrium under the influence of hydration.[20] Table 1 also shows that the zero point vibrational energy (ZPE) correction has a slight effect on the magnitude of the relative energies of the different tautomers while the scaled and unscaled ZPE corrected relative energies have approximately the same relative values.

The calculated equilibrium constant for the tautomerization and relative concentrations of the different tautomers are presented in Table 2. It is found that in the gas phase for the isolated tautomers at the MP2/6-31G(d,p) level of theory the keto-N7H form would be approximately 63.8% and the keto-N9H form would be about 36% while the enol-N9H form would be only about 0.2%. At the HF/6-311++G(d,p) level of theory, there is a slight difference in the relative distribution of the enol-N9H form which is predicted to be about 1.4%. Hydration has an influence on the relative distribution of the tautomers. In the case of monohydrated species, the keto-N9H form is predicted to be about 53.3%, keto-N7H is about 46.5%, and enol-N9H is about 0.2% at the MP2/6-31G(d,p) level. Dihydration further increases the population of the keto-N9H form which is predicted to be about 60%, keto-N7H about 40%, and enol-N9H only about 0.01% at the MP2/6-31G(d,p) level of theory. Thus hydration shifts the tautomeric equilibrium from the keto-N7H form to the keto-N9H form. In the dihydrated form they would be in the ratio of 40% and 60%, respectively. Table 2 also reveals that the HF method slightly favors the population of the keto-N9H form for both the isolated and hydrated forms as compared to the respective values at the MP2 level of theory.

Transition States. The transition state structures corresponding to the keto−enol tautomers of the two prototropic forms

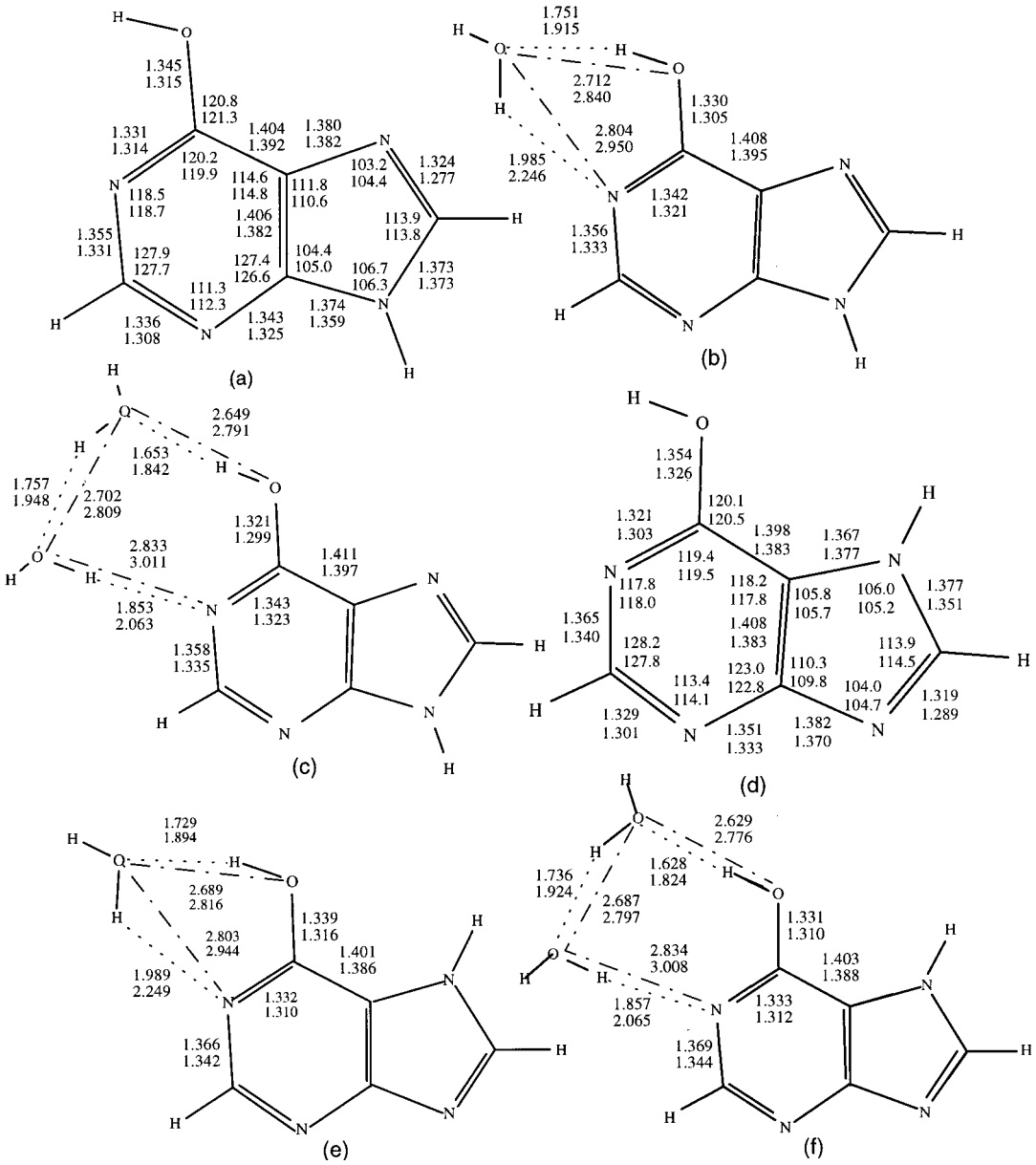

Figure 2. MP2/6-31G(d,p) (top index) and HF/6-311++G(d,p) (bottom index) geometries of hypoxanthine tautomers and hydrated complexes: (a) enol-N9H, (b) enol-N9H·H_2O, (c) enol-N9H·$2H_2O$, (d) enol-N7H, (e) enol-N7H·H_2O and (f) enol-N7H·$2H_2O$. Bond lengths are in angstroms and bond angles are in degrees.

TABLE 1: Relative Total Energies (kcal/mol) of Different Tautomers of Hypoxanthine in the Gas Phase

	HF/6-31G(d,p)				MP2/6-31G(d,p)				HF/6-311++G(d,p)			
complex	ΔE	ΔE^a	ΔE^b	ΔG	ΔE	ΔE^a	ΔE^b	ΔG	ΔE	ΔE^a	ΔE^b	ΔG
keto-N9H	0.0	0.0	0.0	0.0	0.0	0.0	0.0	0.0	0.0	0.0	0.0	0.0
keto-N7H	−0.07	−0.07	−0.07	−0.07	−0.36	−0.32	−0.32	−0.34	−0.25	−0.25	−0.25	−0.26
enol-N9H	1.58	1.45	1.46	1.58	2.98	2.85	2.86	2.96	1.98	1.88	1.89	1.97
enol-N7H	5.27	4.94	4.96	5.27	5.74	5.42	5.43	5.48	5.50	5.18	5.21	5.22
keto-N9H·H_2O	0.0	0.0	0.0	0.0	0.0	0.0	0.0	0.0	0.0	0.0	0.0	0.0
keto-N7H·H_2O	0.45	0.41	0.41	0.45	0.11	0.11	0.11	0.08	0.21	0.16	0.17	0.13
enol-N9H·H_2O	2.81	2.72	2.72	2.81	3.17	3.08	3.09	3.24	3.52	3.52	3.52	3.80
enol-N7H·H_2O	5.63	5.40	5.42	5.63	4.96	4.75	4.76	4.88	6.16	6.02	6.03	6.28
keto-N9H·$2H_2O$	0.0	0.0	0.0	0.0	0.0	0.0	0.0	0.0	0.0	0.0	0.0	0.0
keto-N7H·$2H_2O$	0.75	0.71	0.71	0.75	0.23	0.24	0.24	0.23	0.51	0.48	0.49	0.50
enol-N9H·$2H_2O$	4.70	4.54	4.56	4.70	4.31	4.09	4.10	4.33	5.53	5.41	5.42	5.60
enol-N7H·$2H_2O$	7.17	6.90	6.93	7.17	5.67	5.33	5.34	5.57	7.85	7.62	7.64	7.81

[a] Zero point energy (unscaled) corrected. [b] Zero point energy (scaled) corrected.

(N9H and N7H) of the molecule were computed. The predicted transition states were verified by estabilishing that the Hessians have only one negative eigenvalue. The energetic characteristics of transition states in the gas phase for the isolated, monohydrated, and dihydrated forms of HX at the HF/6-31G(d,p), HF/6-311++G(d,p), MP2/6-31G(d,p)//HF/6-31G(d,p), and MP2/6-311++G(d,p)//HF/6-311++G(d,p) levels of theory are presented in Table 3. These energies were corrected for the zero

TABLE 2: Estimated Equilibrium Constants for Tautomerization *K* (at 298.15 K) and Percentage Relative Concentrations of Tautomers for Selected Equilibria

method	*K*	relative concentration
	keto-N9H ⇆ keto-N7H ⇆ enol-N9H ⇆ enol-N7H	
HF/6-31G(d,p)	1.125, 6.174×10^{-2}, 1.973×10^{-3}	45.56, 51.27, 3.17, 6×10^{-5}
MP2/6-31G(d,p)	1.775, 3.811×10^{-3}, 1.422×10^{-2}	35.95, 63.81, 0.24, 3×10^{-5}
HF/6-311++G(d,p)	1.551, 2.320×10^{-2}, 4.147×10^{-3}	38.65, 59.95, 1.40, 6×10^{-5}
	keto-N9H·H_2O ⇆ keto-N7H·H_2O ⇆ enol-N9H·H_2O ⇆ enol-N7H·H_2O	
HF/6-31G(d,p)	0.468, 1.863×10^{-2}, 8.569×10^{-3}	67.72, 31.69, 0.59, 5×10^{-5}
MP2/6-31G(d,p)	0.874, 4.827×10^{-3}, 6.279×10^{-2}	53.24, 46.52, 0.23, 0.01
HF/6-311++G(d,p)	0.803, 2.041×10^{-3}, 1.521×10^{-2}	55.41, 44.50, 0.09, 1×10^{-5}
	keto-N9H·$2H_2O$ ⇆ keto-N7H·$2H_2O$ ⇆ enol-N9H·$2H_2O$ ⇆ enol-N7H·$2H_2O$	
HF/6-31G(d,p)	0.282, 1.272×10^{-3}, 1.547×10^{-2}	77.98, 21.99, 0.03, 4×10^{-6}
MP2/6-31G(d,p)	0.678, 9.880×10^{-4}, 0.123	59.56, 40.40, 0.04, 5×10^{-5}
HF/6-311++G(d,p)	0.430, 1.827×10^{-4}, 2.399×10^{-2}	69.92, 30.07, 0.01, 1×10^{-6}

TABLE 3: Calculated Barrier Height[a] (kcal/mol) for Hypoxanthine in Keto−Enol Tautomerism

species	HF/6-31G(d,p)	HF/6-311++G(d,p)	MP2/6-31G(d,p)// HF/6-31G(d,p)	MP2/6-311++G(d,p)// HF/6-311++G(d,p)
keto-N9H → TS1	47.94	49.08	35.46	35.66
enol-N9H → TS1	46.48	47.19	32.98	33.98
keto-N7H → TS2	51.44	52.54	38.59	38.69
enol-N7H → TS2	46.40	47.08	33.20	34.08
keto-N9H·H_2O → TS1·H_2O	25.02	27.43	11.65	12.49
enol-N9H·H_2O → TS1·H_2O	22.30	23.91	8.68	10.03
keto-N7H·H_2O → TS2·H_2O	26.33	28.97	12.74	14.0
enol-N7H·H_2O → TS2·H_2O	21.32	23.11	8.14	9.83
keto-N9H·$2H_2O$ → TS1·$2H_2O$	27.59	30.98	12.47	14.89
enol-N9H·$2H_2O$ → TS1·$2H_2O$	23.03	25.56	8.25	10.93
keto-N7H·$2H_2O$ → TS2·$2H_2O$	27.98	31.36	12.41	14.78
enol-N7H·$2H_2O$ → TS2·$2H_2O$	21.77	24.21	7.15	9.69

[a] Zero point energy corrected (scaling factor 0.9135).

point vibrational energy (ZPE) obtained from the HF/6-31G(d,p) and HF/6-311++G(d,p) levels of harmonic vibrational frequency calculations and scaled by a factor of 0.9135. At the HF/6-311++G(d,p) level of theory, the transition state geometries (namely, TS1, TS1·H_2O, and TS1·$2H_2O$ corresponding to proton transfer from the keto-N9H to the enol-N9H form, the keto-N9H·H_2O to the enol-N9H·H_2O form, and the keto-N9H·$2H_2O$ to the enol-N9H·$2H_2O$ form, respectively) are shown in Figure 3, while those of the transition state structures (TS2, TS2·H_2O, and TS2·$2H_2O$) corresponding to proton transfer from the keto to the enol tautomers of the isolated, monohydrated, and dihydrated forms of the N7H prototropic tautomers are presented in Figure 4. The geometric parameters at the HF/6-31G(d,p) level were found to be similar to those obtained at the HF/6-311++G(d,p) level; therefore, they are not presented here. Due to the large size of the studied species, we were not able to optimize the transition state geometries at the electron correlated level. Table 3 shows that the proton transfer is characterized by a high activation energy. Inclusion of a water molecule (monohydration) drastically reduces the activation energy, suggesting that proton transfer would be easily facilitated by the presence of a water molecule. In the crystal of isocytosine, the presence of water vapor increases proton migration, which leads to an increased amount of electric current passing through it.[21] Such phenomena are indicative of the fact that the presence of water vapor decreases the barrier height of proton transfer. For the dihydrated complexes, the proton transfer activation energy is slightly higher than those of the monohydrated complexes (Table 3). The inclusion of the electron correlation effect substantially decreases the height of barrier by more than 12 kcal/mol. Similar results have been found for guanine also.[19a]

The analysis of the transition state geometries of the monohydrated complexes for both of the prototropic tautomers of HX shown in Figures 3 and 4 reveal that the proton attached to the N1 site of HX is migrated toward the water molecule. In the case of dihydrated complexes, in the ground state the two water molecules are hydrogen bonded with each other (Figures 1 and 2). In the transition state a proton is shared equally by both water molecules and is approximately equidistant from them (Figures 3 and 4). Thus, the transition state geometries are of the zwitterionic type having the $H_3O^+\cdots HX^-$ type of structure for the monohydrated forms and the $H_5O_2^+\cdots HX^-$ type of structure for the dihydrated tautomers. The molecular electrostatic potential derived charge analysis from the CHELPG procedure[22] shows that for the monohydrated transition structure with the N9H prototropic form (TS1·H_2O), the H_3O^+ ion has about 0.56 au of positive charge while the same amount of negative charge is found at the hypoxanthine anion at the HF/6-311++G(d,p) level of theory. In the case of the dihydrated transition structure (TS1·$2H_2O$), $H_5O_2^+$ ion has about 0.71 au of positive charge and the same amount of negative charge at the hypoxanthine anion at the same level of theory. Similar results were found for the N7H prototropic complexes also. Thus a charge analysis of the hydrated transition structures shows that the zwitterionic nature is more pronounced in the dihydrated form compared to the monohydrated form. This result is not surprising in view of a recent molecular dynamics simulation study of proton transfer along small water clusters which are protonated linear chains of six water molecules, a linear water chain containing the water molecules, and an amino molecule.[23] The proton transfer process is characterized by many transient states; the proton is found either as proton centered ($H_5O_2^+$) or hydronium centered (H_3O^+) with almost equal probability.[23] Our theoretical prediction is also validated from an experimental work performed on the molecular dynamics of tautomerization of 7-azaindole (7AI) using femtosecond time-of-flight mass spectroscopy by Zewail and co-workers[24] in which they have shown that tautomerization is a two-step process. An intermedi-

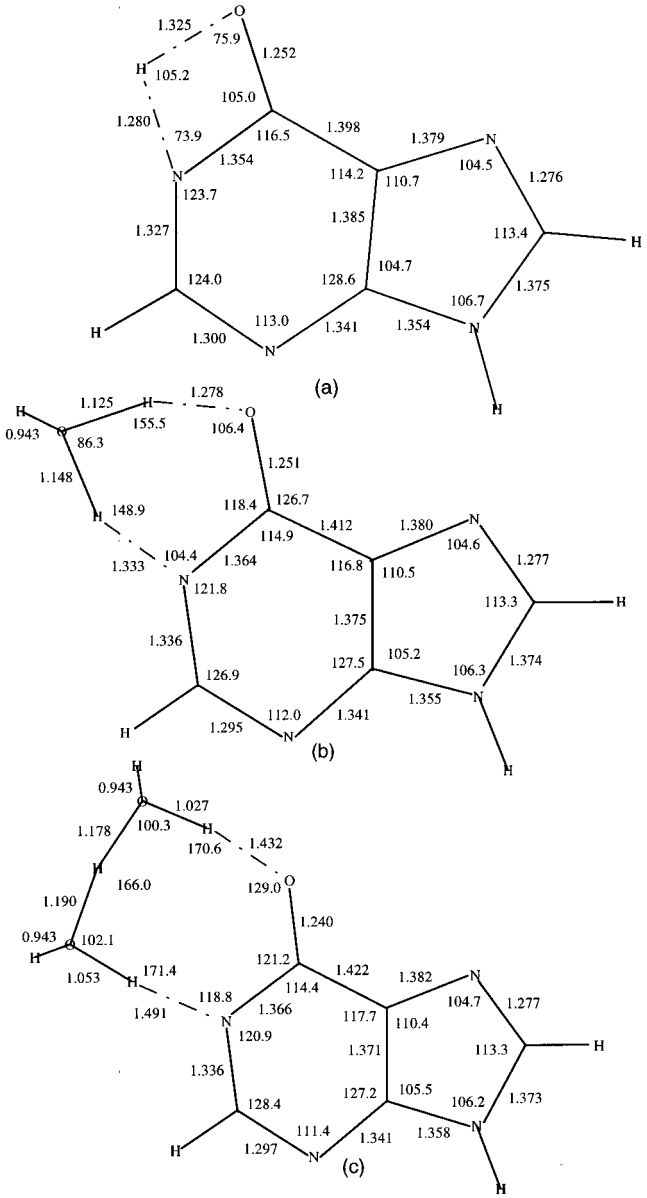

Figure 3. HF/6-311++G(d,p) transition state geometry of (a) TS1 corresponding to the proton transfer from the keto-N9H to the enol-N9H form, (b) TS1·H_2O corresponding to the proton transfer from the keto-N9H·H_2O to the enol-N9H·H_2O form, and (c) TS1·$2H_2O$ corresponding to the proton transfer from the keto-N9H·$2H_2O$ to the enol-N9H·$2H_2O$ form of hypoxanthine. Bond lengths are in angstroms and bond angles are in degrees.

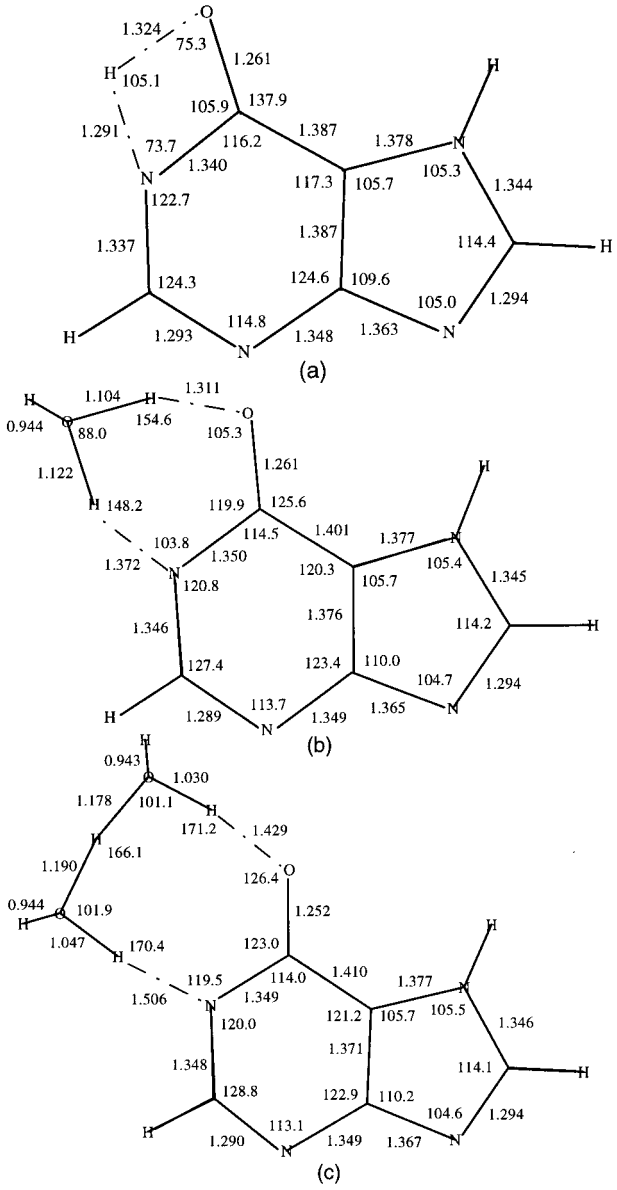

Figure 4. HF/6-311++G(d,p) transition state geometry of (a) TS2 corresponding to the proton transfer from the keto-N7H to the enol-N7H form, (b) TS2·H_2O corresponding to the proton transfer from the keto-N7H·H_2O to the enol-N7H·H_2O form, and (c) TS2·$2H_2O$ corresponding to the proton transfer from the keto-N7H·$2H_2O$ to the enol-N7H·$2H_2O$ form of hypoxanthine. Bond lengths are in angstroms and bond angles are in degrees.

ate zwitterionic form ($7AI^+-7AI^-$) of the 7-azaindole dimer is formed at the first step.

Interaction Energy and Dipole Moments. The basis set superposition error (BSSE) corrected interaction energies were calculated as the energy differences between the hydrated complex and the sum of the isolated monomers in which the energy of the monomer was calculated by adding ghost atoms in the space of the complex corresponding to the equilibrium positions of the counterpart monomer. The BSSE corrected interaction energy presented in Table 4 shows that the keto-N9H form has the highest interaction energy (in magnitude) for both the mono- and dihydrated complexes at the HF/6-31G(d,p) and HF/6-311++G(d,p) levels of theory, while at the MP2/6-31G(d,p) level the enol-N7H form has the highest interaction energy in magnitude, and the keto-N9H form is next to it. For the monohydrated complexes, the interaction energy (in magnitude) lies in the range of 8.2−9.3 kcal/mol, while for dihydrated complexes the range is 17.4−20.2 kcal/mol at the HF/6-31G(d,p) level of theory. At the MP2/6-31G(d,p) level of theory, the interaction energies for the mono- and dihydrated complexes are about 1−4 kcal/mol higher in magnitude than the corresponding value at the HF/6-31G(d,p) level of theory. At the HF/6-311++G(d,p) level, the interaction energies are

TABLE 4: BSSE Corrected Interaction Energy (kcal/mol) of Hydration of Hypoxanthine

species	HF/6-31G(d,p)	MP2/6-31G(d,p)	HF/6-311++G(d,p)
keto-N9H·H_2O	−9.29	−10.18	−8.88
keto-N7H·H_2O	−8.79	−9.74	−8.43
enol-N9H·H_2O	−8.21	−10.04	−7.29
enol-N7H·H_2O	−9.10	−11.03	−8.18
keto-N9H·$2H_2O$	−20.14	−22.34	−18.55
keto-N7H·$2H_2O$	−19.32	−21.73	−17.79
enol-N9H·$2H_2O$	−17.43	−21.52	−15.41
enol-N7H·$2H_2O$	−18.76	−23.17	−16.66

TABLE 5: Gas Phase Dipole Moments (debyes) of Hypoxanthine and Its Hydrated Complexes

species	HF/6-31G(d,p)	MP2/6-31G(d,p)	HF/6-311++G(d,p)
keto-N9H	5.60	4.98	5.72
keto-N7H	1.58	2.10	1.47
enol-N9H	2.50	2.61	2.59
enol-N7H	5.21	5.09	5.22
keto-N9H·H_2O	4.44	4.22	3.98
keto-N7H·H_2O	3.11	3.38	3.27
enol-N9H·H_2O	3.47	3.58	3.22
enol-N7H·H_2O	4.28	4.25	4.33
keto-N9H·$2H_2O$	3.68	3.45	3.62
keto-N7H·$2H_2O$	3.28	3.55	3.34
enol-N9H·$2H_2O$	2.94	3.04	2.77
enol-N7H·$2H_2O$	4.12	4.10	4.24
TS1	4.80		4.84
TS1·H_2O	3.65		3.70
TS1·$2H_2O$	3.11		3.32
TS2	2.95		2.92
TS2·H_2O	4.26		4.33
TS2·$2H_2O$	6.32		6.66

about 1−2 kcal/mol lower in magnitude than the corresponding value at the HF/6-31G(d,p) level of theory (Table 4). Generally the interaction energy correlates well with the hydrogen bonding strength; the data presented in Table 4 show that the hydrogen bonding strength in the complexes of keto-N9H would be more than the other tautomeric forms at the HF level of theory while at the MP2 level it would be next to the enol-N7H tautomeric form.

The dipole moments of the isolated and hydrated forms of hypoxanthine tautomers and their transition states corresponding to the keto and enol forms presented in Table 5 show that, for the isolated forms, keto-N9H has the highest while keto-N7H has the lowest dipole moment except at the MP2 level where the enol-N7H form is about 0.1 D higher than the keto-N9H form. The higher dipole moment reflects better solvation in the polar environment. Thus, in polar media, the keto-N9H form would stabilize more. The higher dipole moment of the keto-N9H form and lower dipole moment of the keto-N7H tautomer explain the preferential stability of the keto-N9H form on the mono- and dihydration. Hydration leads to a decrease in the dipole moment for the keto-N9H form and an increase for the keto-N7H form of HX. For the N9H prototropic tautomers, hydration leads to a decrease in the dipole moments for the transition states. The reverse is true for N7H prototropic tautomers.

Conclusion

Hydration has an appreciable effect on the relative distribution of different tautomers and on the structure of the transition states corresponding to the proton transfer from the keto to the enol tautomeric form of the hypoxanthine. At the MP2/6-31G(d,p) level of theory, it has been predicted that hypoxanthine would be present mainly in the two keto prototropic tautomeric forms: the relative distribution would be such that the keto-N7H form would be about 63.8%, keto-N9H would be about 36%, and the enol-N9H form would be only about 0.2%. Hydration leads to a shift in the tautomeric equilibria toward the keto-N9H form. In the case of monohydration, the keto-N9H form would be about 53.3%, the keto-N7H form about 46.5%, and the enol-N9H form about 0.2%. Dihydration further increases the population of the keto-N9H form, which is predicted to be about 60%, the keto-N7H form about 40%, and the form enol-N9H only about 0.01%. The transition state structures corresponding to the proton transfer from the hydrated keto form to the hydrated enol prototropic tautomers are predicted to be zwitterionic in nature having the structure of the $H_3O^+\cdots HX^-$ type for the monohydrated forms and of the $H_5O_2^+\cdots HX^-$ type for the dihydrated forms of hypoxanthine.

Acknowledgment. The authors are thankful to NIH-RCMI Grant G1 2RR13459-21, NSF-CREST Grant 9805465, and ONR Grant N00014-98-1-0592 for financial assistance.

References and Notes

(1) (a) Watson, J. D.; Crick, F. H. C. *Nature* **1953**, *171*, 737. (b) Lowdin, P. O. *Adv. Quantum Chem.* **1965**, *2*, 213.

(2) (a) Vranken, H.; Smets, J.; Maes, G.; Lapinski, L.; Nowak, M. J.; Adamowicz, L. *Spectrochim. Acta* **1994**, *50A*, 875. (b) Kwiatkowski, J. S.; Leszczynski, J. *Int. J. Quantum Chem.* **1997**, *61*, 453. (c) Leszczynski, J. *J. Mol. Struct. (THEOCHEM)* **1994**, *311*, 37. (d) Shukla, M. K.; Mishra, P. C. *Spectrochim. Acta A* **1996**, *52*, 1547. (e) Broo, A.; Holmen, A. *J. Phys. Chem. A* **1997**, *101*, 3589. (f) Chenon, M.-T.; Pugmire, R. J.; Grant, D. M.; Panzica, R. P.; Townsend, L. B. *J. Am. Chem. Soc.* **1975**, *97*, 4627. (g) Leszczynski, J. *J. Phys. Chem.* **1993**, *97*, 3520. (h) Sponer, J.; Leszczynski, J. *Struct. Chem.* **1995**, *6*, 281. (i) Shukla, M. K.; Mishra, P. C. *J. Mol. Struct.* **1994**, *324* 241. (j) Chandra, A. K.; Nguyen, M. T.; Uchimaru, T.; Zeegers-Huyskens, T. *J. Phys. Chem. A* **1999**, *103*, 8853.

(3) Stryer, L. *Biochemistry*, 3rd ed Freeman: New York, 1988.

(4) (a) Holley, R. W.; Apgar, J.; Everett, G. A.; Madison, J. T.; Marquisee, M.; Merrill, S. H.; Penswick, J. R.; Zamir, A. *Science* **1965**, *147*, 1462. (b) Dutting, D.; Karau, W.; Melchers, F.; Zachau, H. G. *Biochim. Biophys. Acta* **1965**, *108*, 194. (c) Grunberger, D.; Holy, A.; Sorm, F. *Biochim. Biophys. Acta* **1967**, *134*, 484.

(5) Hernandez, B.; Luque, F. J.; Orozco, M. *J. Org. Chem.* **1996**, *61*, 5964.

(6) Nonella, M.; Hanggi, G.; Dubler, E. *J. Mol. Struct. (THEOCHEM)* **1993**, *279*, 173.

(7) Sheina, G. G.; Stepanian, S. G.; Radchenko, E. D.; Blagoi, Yu. P. *J. Mol. Struct.* **1987**, *158*, 275.

(8) Lin, J.; Yu, C.; Peng, S.; Akiyama, I.; Li, K.; Lee, L. K.; LeBreton, P. R. *J. Phys. Chem.* **1980**, *84*, 1006.

(9) Costas, M. E.; Acevedo-Chavez, R. *J. Phys. Chem. A* **1997**, *101*, 8309.

(10) El-Bakali Kassimi, N.; Thakkar, A. J. *J. Mol. Struct. (THEOCHEM)* **1996**, *366*, 185.

(11) Kyogoku, Y.; Lord, R. C.; Rich, A. *Biochim. Biophys. Acta* **1969**, *179*, 10.

(12) Ohta, Y.; Nishimoto, K.; Tanaka, H.; Baba, Y.; Kagemoto, A. *Bull. Chem. Soc. Jpn.* **1989**, *62*, 2441.

(13) Munns, A. R. I.; Tollin, P. *Acta Crystallogr. B* **1970**, *26*, 1101.

(14) Lichtenberg, D.; Bergmann, F.; Neiman, Z. *Isr. J. Chem.* **1972**, *10*, 805.

(15) Chenon, M. T.; Pugmire, R. J.; Grant, D. M.; Panzica, R. P.; Townsend, L. B. *J. Am. Chem. Soc.* **1975**, *97*, 4636.

(16) (a) Gorb, L.; Leszczynski, J. In *Computational Molecular Biology*; Leszczynski, J., Ed.; Theoretical Computational Chemistry 8; Elsevier Science: New York, 1999; p 167. (b) Schneider, B.; Berman, H. *Biophys. J.* **1995**, *69*, 2661. (c) Chahinian, M.; Seba, H. B.; Ancian, B. *Chem. Phys. Lett.* **1998**, *285*, 337. (d) Schneider, B.; Cohen, D.; Barman, H. *Biopolymers* **1992**, *32*, 725.

(17) *Exploring Chemistry with Electronic Structure Methods*, 2nd ed.; Foresman, J. B., Frisch, A., Eds.; Gaussian Inc.: Pittsburgh, PA, 1996.

(18) Frisch, M. J.; Trucks, G. W.; Schlegel, H. B.; Gill, P. M. W.; Johnson, B. G.; Robb, M. A.; Cheeseman, J. R.; Keith, T.; Petersson, G. A.; Montgomery, J. A.; Raghavachari, K.; Al-Laham, M. A.; Zakrzewski, V. G.; Ortiz, J. V.; Foresman, J. B.; Cioslowski, J.; Stefanov, B. B.; Nanayakkara, A.; Challacombe, M.; Peng, C. Y.; Ayala, P. Y.; Chen, W.; Wong, M. W.; Andres, J. L.; Replogle, E. S.; Gomperts, R.; Martin, R. L.; Fox, D. J.; Binkley, J. S.; Defrees, D. J.; Baker, J.; Stewart, J. P.; Head-Gordon, M.; Gonzalez, C.; Pople, J. A. *Gaussian 94*, Revision E.2; Gaussian, Inc.: Pittsburgh, PA, 1995.

(19) (a) Gorb, L.; Leszczynski, J. *J. Am. Chem. Soc.* **1998**, *120*, 5024. (b) Shukla, M. K.; Leszczynski, J. *Int. J. Quantum Chem.* **2000**, *77*, 240. (c) Gorb, L.; Podolyan, Y.; Leszczynski, J. *J. Mol. Struct. (THEOCHEM)* **1999**, *487*, 47. (d) Gu, J.; Leszczynski, J. *J. Phys. Chem. A* **1999**, *103*, 2744. (e) Gorb, L.; Leszczynski, J. *Int. J. Quantum Chem.* **1998**, *70*, 855.

(20) (a) Smets, J.; Adamowicz, L.; Maes, G. *J. Mol. Struct.* **1994**, *322*, 113. (b) Buyl, F.; Smets, J.; Maes, G.; Adamowicz, L. *J. Phys. Chem.* **1995**, *99*, 14967. (c) Smets, J.; Destexhe, A.; Adamowicz, L.; Maes, G. *J. Phys. Chem. A* **1998**, *102*, 8157.

(21) (a) Skaric, V.; Lacan, G.; Skaric, D. *J. Chem. Soc., Perkin Trans 1* **1977**, 757. (b) Thomas, J. M.; Evans, J. R. N.; Lewis, T. J. *Discuss. Faraday Soc.* **1971**, *51*, 73.

(22) Breneman, C. M.; Wiberg, K. B. *J. Comput. Chem.* **1990**, *11*, 361.

(23) Sadeghi, R. R.; Cheng, H.-P. *J. Chem. Phys.* **1999**, *111*, 2086.

(24) Douhal, A.; Kim, S. K.; Zewail, A. H. *Nature (London)* **1995**, *378*, 260.